Biophysical Journal, Volume *115*

Supplemental Information

Synchronization of Triggered Waves in Atrial Tissue

Yohannes Shiferaw, Gary L. Aistrup, and John A. Wasserstrom

Online Supplement

Phenomenological model equations

Ca concentration equations

To model the dynamics of Ca we divide the cell interior into compartments that represent various intracellular spaces. These spaces are illustrated in Figure 1D and described in detail in the main text. The total Ca concentration in each compartment obeys the Ca flux equations:

$$v_b \frac{dc_b^T}{dt} = J_r^b - J_{up}^b - J_{Ca} + J_{NaCa} - J_{bi}, \tag{1}$$

$$v_{srb} \frac{dc_{srb}^T}{dt} = -J_r^b + J_{up}^b - J_{bsr}, \tag{2}$$

$$v_i \frac{dc_i^T}{dt} = J_r^i - J_{up}^i + J_{bi}, \tag{3}$$

$$v_{jsr} \frac{dc_{jsr}^T}{dt} = -J_r^i + J_{ni}, \tag{4}$$

$$v_{nsr} \frac{dc_{nsr}^T}{dt} = J_{up}^i - J_{ni} + J_{bsr} \ . \tag{5}$$

The definition of each of these currents is given in Table 1 in the main text. For convenience we rescale the boundary and interior currents to the volume of the respective cytosol and make the replacements:

$$\frac{J_r^b}{v_b} \to J_r^b \ , \quad \frac{J_{up}^b}{v_b} \to J_{up}^b , \quad \frac{J_{NaCa}}{v_b} \to J_{NaCa} , \quad \frac{J_{Ca}}{v_b} \to J_{Ca} \ , \quad \frac{J_{bi}}{v_b} \to J_{bi} \tag{6}$$

$$\frac{J_r^i}{v_i} \to J_r^i \ , \quad \frac{J_{up}^i}{v_i} \to J_{up}^i \ . \tag{7}$$

The equations are now written with the rescaled currents as

$$\frac{dc_b^T}{dt} = J_r^b - J_{up}^b - J_{Ca} + J_{NaCa} - J_{bi}, \tag{8}$$

$$\frac{dc_{srb}^T}{dt} = \left(\frac{v_b}{v_{srb}}\right)\left(-J_r^b + J_{up}^b\right) - \left(\frac{1}{v_{srb}}\right) J_{bsr}, \tag{9}$$

$$\frac{dc_i^T}{dt} = J_r^i - J_{up}^i + \left(\frac{v_b}{v_i}\right) J_{bi} \ , \tag{10}$$

$$\frac{dc_{jsr}^T}{dt} = \left(\frac{v_i}{v_{jsr}}\right)\left(-J_r^i\right) + \left(\frac{1}{v_{jsr}}\right) J_{ni} \ , \tag{11}$$

$$\frac{dc_{nsr}^T}{dt} = \left(\frac{v_i}{v_{nsr}}\right)J_{up}^i - \left(\frac{1}{v_{nsr}}\right)J_{ni} + \left(\frac{1}{v_{nsr}}\right)J_{bsr}\,. \tag{12}$$

Note here that all current fluxes are now in units of $\mu M/ms$. It is also convenient to rescale the diffusive currents

$$\frac{J_{bsr}}{v_{srb}} \to J_{bsr}\ ,\ \ \frac{J_{ni}}{v_{jsr}} \to J_{ni}\ . \tag{13}$$

So we can write the final equations as

$$\frac{dc_b^T}{dt} = J_r^b - J_{up}^b - J_{Ca} + J_{NaCa} - J_{bi}, \tag{14}$$

$$\frac{dc_{srb}^T}{dt} = \left(\frac{v_b}{v_{srb}}\right)\left(-J_r^b + J_{up}^b\right) - J_{bsr}, \tag{15}$$

$$\frac{dc_i^T}{dt} = J_r^i - J_{up}^i + \left(\frac{v_b}{v_i}\right)J_{bi}\,, \tag{16}$$

$$\frac{dc_{jsr}^T}{dt} = \left(\frac{v_i}{v_{jsr}}\right)\left(-J_r^i\right) + J_{ni}\,, \tag{17}$$

$$\frac{dc_{nsr}}{dt} = \left(\frac{v_i}{v_{nsr}}\right)J_{up}^i - \left(\frac{v_{jsr}}{v_{nsr}}\right)J_{ni} + \left(\frac{v_{srb}}{v_{nsr}}\right)J_{bsr}\ . \tag{18}$$

The diffusive fluxes between compartments are given by

$$J_{bi} = \frac{c_b - c_i}{\tau_{bi}}\ , \tag{19}$$

$$J_{bsr} = \frac{c_{srb} - c_{nsr}}{\tau_{sbi}}, \tag{20}$$

$$J_{ni} = \frac{c_{nsr} - c_{jsr}}{\tau_{si}}, \tag{21}$$

where τ_{bi} is the diffusion time scale linking the boundary and interior cytosol, τ_{sbi} is the time scale governing diffusion from the internal to boundary SR volumes, and τ_{si} is the diffusional delay from interior NSR to JSR.

Buffers

If c_x^T denotes the total Ca concentration in compartment x, c_x denotes the free concentration, B is the total buffer concentration, and $[CaB]$ is the concentration of bound buffers then:

$$\frac{d[CaB]}{dt} = k_{on}c_x(B - [CaB]) - k_{off}[CaB], \tag{22}$$

where k_{on} and k_{off} is the binding and dissociation rate respectively. For simplicity we assume instantaneous buffering so that the bound Ca is at steady state is

$$[CaB] = \frac{Bc_x}{c_x + K}\ , \tag{23}$$

where $K = k_{on}/k_{off}$. Therefore, given the presence of multiple buffers with total concentration B_i and kinetics K_i, the total Ca in the cell is given by

$$c_x^T = c_x + \sum_i \frac{B_i c_x}{K_i + c_x} \quad . \tag{24}$$

In this study we will apply two instantaneous cytosolic buffers. These are Calmodulin buffers with $B_{CaM} = 24.0\mu M$ and $K_{CaM} = 7.0$, and SR buffers with $B_{SR} = 47.0\mu M$ and $K_{SR} = 0.6$. An advantage of solving directly for the total Ca concentrations (Eqs. 14-18) is that all internal Ca fluxes cancel exactly. Previous approaches to instantaneous buffering did not enforce this exact cancellation and can lead to unphysical fluxes which violate ion conservation. However, to apply these equations it is necessary to compute the free from total Ca concentration. To do this it is necessary to invert Eq. (24). However, since Eq. (24) is nonlinear we will first fit the curve to a simpler function of the form

$$c_x^T = a_1 c_x + \frac{a_2 c_x}{a_3 + c_x} \quad . \tag{25}$$

Fitting the buffers for concentrations in the physiological range $0.1\mu M \le c_x \le 5\mu M$ gives a solution $a_1 = 2.23895, a_2 = 52.0344, a_3 = 0.666509$. Inverting Eq. (25) yields the free concentration

$$c_x = \frac{1}{2a}\left(-a_2 - a_1 a_3 + c_x^T + \sqrt{(a_2 + a_1 a_3 - c_x^T)^2 + 4a_1 a_3 c_x^T}\right) \quad . \tag{26}$$

Therefore, at each time step we use Eq. (26) to compute the free Ca concentration that regulates the Ca fluxes.

The volume factors

In order to solve the Ca flux equations it is necessary to determine the volume ratios given in Eqs (14-18). To estimate these factors we first note that an atrial myocyte has an approximate volume of $V_{Cell} \sim 15\mu m \times 15\mu m \times 60\mu m$. The boundary region will have a thickness of roughly $1.0\mu m$, so that the volume of the interior $V_i \sim 13\mu m \times 13\mu m \times 58\mu m$, which gives a ratio of boundary to interior of roughly $(V_{cell} - V_i)/V_i \sim 0.4$. Thus, the ratio of cytosolic volumes between the boundary and interior should be approximately in the range $\sim 0.1 - 0.6$. In this study we will use a ratio $v_b/v_i = 0.3$. To determine volume ratios with the SR we follow Restrepo et al. (1) who estimated that in ventricular myocytes the SR volume is roughly 30 times smaller than the cytosol. We assume that this also applies in atrial myocytes at both the boundary and the interior spaces so that $v_b/v_{srb} = 30$, and $v_i/v_{nsr} = 30$. Also, we assume that the NSR and JSR are roughly the same volume so that $v_{jsr}/v_{nsr} = 1$, and $v_i/v_{jsr} = 30$. Finally, we set $v_{srb}/v_{nsr} = 0.3$, since the volume ratio of the boundary and interior SR should proportional to the ratio of total available volume.

The number of RyR clusters available

To estimate the number of available RyR clusters we treat the cell as an approximately 3D rectangular grid. Assuming a $\sim 1\mu m$ spacing we estimate that there are roughly ~ 5000 boundary sites and ~ 10000 interior sites. However, since we expect that RyR clusters are non-uniform we expect a lesser number of junctional and non-junctional sites. In this study we will use $N_b = 2500$ and $N_i = 4000$.

Spark rate parameters

The boundary spark recruitment rate is given by

$$\alpha_b = a_b P_O |i_{Ca}| \Phi(c_{srb}) \tag{27}$$

where a_b is a constant, P_O is the proability of beingin the state O, i_{Ca} is the current through the LCC channel, and

$$\Phi(c_{srb}) = \frac{1}{1 + \left(\frac{c_{srb}^*}{c_{srb}}\right)^{\gamma_1}} \ . \tag{28}$$

The interior spark rate is

$$\alpha_i = \left(a_i \ F(p_b) + b_i \, G(p_i)\right)\phi\left(c_{jsr}\right), \tag{29}$$

where

$$\phi\left(c_{jsr}\right) = \frac{1}{1 + \left(\frac{c_{jsr}^*}{c_{jsr}}\right)^{\gamma_2}} \ , \tag{30}$$

$$F(p_b) = \frac{1}{1 + \left(\frac{p_b^*}{p_b}\right)^{\gamma_b}}, \tag{31}$$

$$G(p_i) = \frac{1}{1 + \left(\frac{p_i^*}{p_i}\right)^{\gamma_i}} \ . \tag{32}$$

All parameters used in the model are given in Table (3).

The sodium-calcium exchange current

In this study we use a standard formulation of I_{NaCa} (2).

$$I_{NaCa} = A_{NaCa}\left(\frac{Na_i^3 Ca_o \exp(0.35z) - Na_o^3 c_b \exp\left((-0.65z)\right)}{(1 + 0.2\exp(-0.65z))U}\right) \tag{33}$$

where $z = VF/RT$, and where

$$A_{NaCA} = \frac{1}{1 + \left(\frac{0.3}{c_b}\right)^3} \ , \tag{34}$$

$$U = K_{m,Cao}Na_i^3 + K_{m,Nao}^3 c_b + K_{m,Nai}^3 Ca_o \left(1 + \frac{c_b}{K_{m,Cai}}\right)$$
$$+K_{m,Cai}Na_o^3 \left(1 + \left(\frac{Na_i}{K_{m,Nai}}\right)^3\right) + Na_i^3 Ca_o + Na_o^3 c_b \,. \quad (35)$$

Model parameters used are: $K_{m,Cao} = 1.3mM, K_{m,Cai} = 0.0036mM, K_{m,Nai} = 12.3mM, K_{m,Nao} = 87.5mM$. Concentration parameters are given in Table 4.

The L-type Ca current

We use a standard formulation of the LCC current. The driving force is given by

$$i_{Ca} = 4P_{Ca}zF\frac{c_b \exp(2z) - 0.341Ca_o}{\exp(2z) - 1}\,, \quad (36)$$

where $z = VF/RT$. The open probability is governed my the Markov state diagram shown in Figure (3) which is solved in the deterministic limit. The Ca independent transition rates are given by:

$$\alpha = \frac{1}{1 + \exp\left(-\frac{V}{4}\right)}\,, \quad (37)$$
$$\beta = 1 - \alpha, \quad (38)$$
$$r_2 = 3.0, \quad (40)$$
$$k_1 = 0.00224, \quad (41)$$
$$P_3 = \frac{1}{1 + \exp\left(-\frac{V+40}{3}\right)}, \quad (42)$$
$$k_3 = \frac{1 - P_3}{3}, \quad (43)$$
$$P_r = 1 - \frac{1}{1 + \exp\left(-\frac{V+40}{4}\right)}\,, \quad (44)$$
$$R = 10 + 4954\exp\left(\frac{V}{15.6}\right), \quad (45)$$
$$\tau_{Ba} = (R - 450)P_r + 450\,, \quad (46)$$
$$P = \frac{1}{1 + \exp\left(-\frac{(V+40)}{10}\right)}\,, \quad (47)$$
$$k_6 = \frac{P}{\tau_{Ba}}, \quad (48)$$
$$k_5 = \frac{1 - P}{\tau_{Ba}}\,. \quad (49)$$

The Ca dependent transition rates are

$$s_1 = 0.00195 + 0.06 f_{Ca}, \tag{50}$$

$$k_2 = 0.00413 + 0.06 f_{Ca}, \tag{51}$$

where the Ca dependence is given by

$$f_{Ca} = \frac{1}{1 + \left(\frac{c'}{c_b}\right)^2} \quad , \tag{52}$$

and where $c' = 0.2\mu M$ is the diastolic Ca concentration. All transition rates between states facing a Ca spark are identical with the exception of the Ca transition rates, for which we set $f_{ca} = 1$. This is because the Ca concentration in the vicinity of LCC channels during a Ca should be $\sim 100\mu M$, which will saturate the Ca dependence of the LCC channel. The total open probability is given by the two components

$$P_t = P_o + P_{os}\,, \tag{53}$$

so that we can write the total LCC current as $I_{Ca} = P_t \cdot i_{Ca}$.

Sodium concentration

To model the changes in internal sodium concentration we use a function $Na_i(T)$ giving sodium concentration as a function of the pacing period T. In this study we use a simple linear depenence so that $Na_i = 12mM$ at a pacing period of $T = 500ms$, and $Na_i = 14mM$ at faster pacing rates of $T = 250ms$. This gives a functional form

$$Na_i(T) = 16mM - \frac{T}{125\ ms} \quad . \tag{54}$$

Ca cycling fluxes

The explicit Ca cycling fluxes used in Eqs (14-18) are given bellow:

$$J_r^b = g_b c_{srb} p_b, \tag{55}$$

$$J_r^i = g_i c_{sri} p_i, \tag{56}$$

$$J_{up}^b = \frac{g_{up}^b c_b^3}{c_b^3 + c_b^{*3}}, \tag{57}$$

$$J_{up}^i = \frac{g_{up}^i c_i^3}{c_i^3 + c_i^{*3}}, \tag{58}$$

$$J_{Ca} = g_{Ca} I_{Ca}, \tag{59}$$

$$J_{NaCa} = g_{NaCa} I_{NaCa}\ . \tag{60}$$

Explicit parameters used for each current are given in Table (1).

Computer simulation times

We have coupled our Ca cycling model with the major ion currents in the Grandi human action potential model (3). The full model consists of 27 differential equations which we solve using a time step of $\Delta t = 0.05ms$. Simulations

of a single cell paced at $CL = 250ms$ for 100 beats requires $0.4s$ of simulation time using a single processor (Intel Xeon E5-2667 v3 3.20GHz). Simulation of 100 beats at the same rate on a 400 cell cable requires 4 minutes of simulation time.

Detailed 3D cell model simulations

In this study we develop a phenomenological Ca cycling model in atrial myocytes. To justify the various functional forms used for the spark recruitment rate we rely on a spatially distributed model of atrial myocytes developed previously by the authors(4). This model is based on a model due to Restrepo et al. (1, 5) in which the cardiac myocyte is represented as a 3D array of subcellular compartments that are diffusively coupled. Full details of the model framework and parameters have been given in our previous study (4). In the simulations performed in Figure 2A-D our cardiac cell model consists of 60 planes representing Z-planes, where each plane contains an array of 20×20 regularly spaced compartments. All sites at the boundary of the cell are designated as junctional CRUs, while all other sites are non-junctional CRUs. In this study we consider the dynamics of Ca cycling when the cell is paced with an AP clamp. Our AP clamp is taken to have the functional form (6) given by

$$V(t) = \begin{cases} V_{min} + (V_{max} - V_{min})\sqrt{1 - ((t - mCL)/xCL)^2} & mCL \le t \le mCL + xCL \\ V_{min} & mCL + xCL < t < (m+1)CL \end{cases} \quad (61)$$

which mimics a typical AP wave form. Here, the variable CL denotes the pacing cycle length, m is an integer denoting the m^{th} paced beat, and $x = APD/CL$. Following previous studies (6) we let this ratio vary with pacing rate according to the functional form $x = a/(a + CL)$ where $a = 2/3$.

In Figure S1 we show an example of Ca transient alternans in our 3D computational cell model. In this case we have paced the cell to steady state at $CL = 250ms$. The top trace shows the total average Ca concentration in the cell showing an alternating release pattern. Figures (a-d) show two dimensional cross sections of the cell at the beats indicated by the red arrows. Here, we see that during alternans the cell exhibits a pattern of triggered wave propagation on alternate beats. In this case we find that the small Ca transient corresponds to a boundary Ca release, while the large Ca transient corresponds to triggered waves that originates at multiple sites on the cell boundary. In Figure S2 we show line scan images of triggered wave alternans in an isolated atrial myocyte from a failing dog heart. An expanded line scan image of the 5Hz pacing regime shows that Ca release occurs only on alternate beats. In this case we find that the linescan image of the released beat exhibits a standard U-shape release pattern. This indicates that there are multiple release sites on the cell boundary so that Ca propagates inward as a centripetal wave. Thus, the line ends are activated first followed by the center of the cell, which leads to the observed activation pattern.

Full details of the experimental methods are given in Aistrup et al. (7). A more detailed analysis of this dynamical pattern will be presented in a future publication.

ACKNOWLEDGEMENTS

YS thanks Enric Alvarez-Lacalle for useful discussions, and specifically suggesting the approach to buffering used here.

Figures

Figure S1. Triggered wave alternans observed in our 3D computational cell model of an atrial myocyte. Top trace shows the global average Ca concentration in the cell. Bottom figures show two dimensional cross sections at (a) 20ms after the 3rd beat. (b) 100ms after the beginning of the 4th beat. (c) 20ms after the 5th beat. (d) 100ms after the 6th beat. Model parameters are taken from Shiferaw et al.(4).

Figure S2. Example of triggered wave alternans in an isolated atrial myocyte from failing dog heart. During 2Hz pacing, individual subcellular triggered waves begin to develop, whereupon 3.3Hz pacing manifest across the entire length of the cell, and upon 5Hz pacing become essentially severe concordant 'whole-cell' Ca alternans (although, individual triggered waves are still apparent therein). Bottom figure shows an expanded view of the 5Hz pacing interval. Vertical dashed lines indicate 5Hz cycle markers.

Tables

1. Ca cycling flux parameters

Parameter	Description	Value
g_b	Strength of boundary release.	$0.004\ (ms)^{-1}$
g_i	Strength of release from interior sites RyR clusters	$0.015\ (ms)^{-1}$
g_{up}^{b}	Boundary uptake strength	$0.3\mu M/ms$
g_{up}^{i}	Internal uptake strength	$0.1\mu M/ms$
c_b^*	Boundary uptake threshold	$0.3\mu M$
c_i^*	Internal uptake threshold	$0.3\mu M$
g_{Ca}	L-type Ca current flux amplitude	$224\mu M(ms)^{-1}(pA)^{-1}$
g_{NaCa}	Sodium-Calcium exchanger flux amplitude	$2\ \mu M(ms)^{-1}(pA)^{-1}$

2. Diffusion time scales

Parameter	Description	Value
τ_{bi}	Diffusion time between boundary and internal cytosol	$10ms$
τ_{sbi}	Diffusion time between boundary NSR and internal NSR	$10ms$
τ_{si}	Diffusion time between internal NSR and JSR	$50ms$

3. Spark rate parameters

Parameter	Description	Value
a_b	Boundary spark rate constant	$100sparks/(ms \cdot pA)$
γ_1	Hill coefficient for SR load dependence of boundary spark rate	6
c_{srb}^*	Threshold for spark activation at junctional sites	$900\mu M$
γ_2	Hill coefficient for SR load dependence of internal spark rate	4
c_{jsr}^*	Threshold for spark activation at non-junctional sites	$900\mu M$
a_i	Constant that determines contribution of junctional sites to internal spark rate	$0.01sparks/ms$
b_i	Constant that determines strength of spark generation due to Ca waves	$0.2\ sparks/ms$
p_b^*	Threshold for boundary activation of interior sparks	0.5
γ_b	Hill coefficient for boundary spark activation of interior Ca sparks	8
p_i^*	Threshold for internal Ca sparks	0.05
γ_i	Hill coefficient describing Ca wave nucleation	5
β_b	Spark extinction rate at the cell boundary	$1/20\ ms$
β_i	Spark extinction rate in the cell interior	$1/50ms$

4. Constant parameters

Parameter	Description	Value
Na_o	External sodium concentration	$136mM$
Ca_o	External Ca concentration	$1.8mM$
K_o	External potassium concentration	$5.4mM$
K_i	Internal potassium concentration	$140mM$
T	Temperature	$308K$
F	Faraday's constant	$96.485C/mmol$

R	Universal gas constant	$8.315 J(mol\ K)^{-1}$
P_{Ca}	LCC Permeability constant	$5.4 \times 10^{-4}\ cm/s$

References

1. Restrepo, J. G., J. N. Weiss, and A. Karma. 2008. Calsequestrin-mediated mechanism for cellular calcium transient alternans. Biophysical journal 95:3767-3789.
2. Luo, C. H., and Y. Rudy. 1994. A dynamic model of the cardiac ventricular action potential. I. Simulations of ionic currents and concentration changes. Circulation research 74:1071-1096.
3. Grandi, E., S. V. Pandit, N. Voigt, A. J. Workman, D. Dobrev, J. Jalife, and D. M. Bers. 2011. Human atrial action potential and Ca2+ model: sinus rhythm and chronic atrial fibrillation. Circulation research 109:1055-1066.
4. Shiferaw, Y., G. L. Aistrup, and J. A. Wasserstrom. 2017. Mechanism for Triggered Waves in Atrial Myocytes. Biophysical journal 113:656-670.
5. Restrepo, J. G., and A. Karma. 2009. Spatiotemporal intracellular calcium dynamics during cardiac alternans. Chaos 19:037115.
6. Shiferaw, Y., M. A. Watanabe, A. Garfinkel, J. N. Weiss, and A. Karma. 2003. Model of intracellular calcium cycling in ventricular myocytes. Biophysical journal 85:3666-3686.
7. Aistrup, G. L., R. Arora, S. Grubb, S. Yoo, B. Toren, M. Kumar, A. Kunamalla, W. Marszalec, T. Motiwala, S. Tai, S. Yamakawa, S. Yerrabolu, F. J. Alvarado, H. H. Valdivia, J. M. Cordeiro, Y. Shiferaw, and J. A. Wasserstrom. 2017. Triggered intracellular calcium waves in dog and human left atrial myocytes from normal and failing hearts. Cardiovascular research 113:1688-1699.

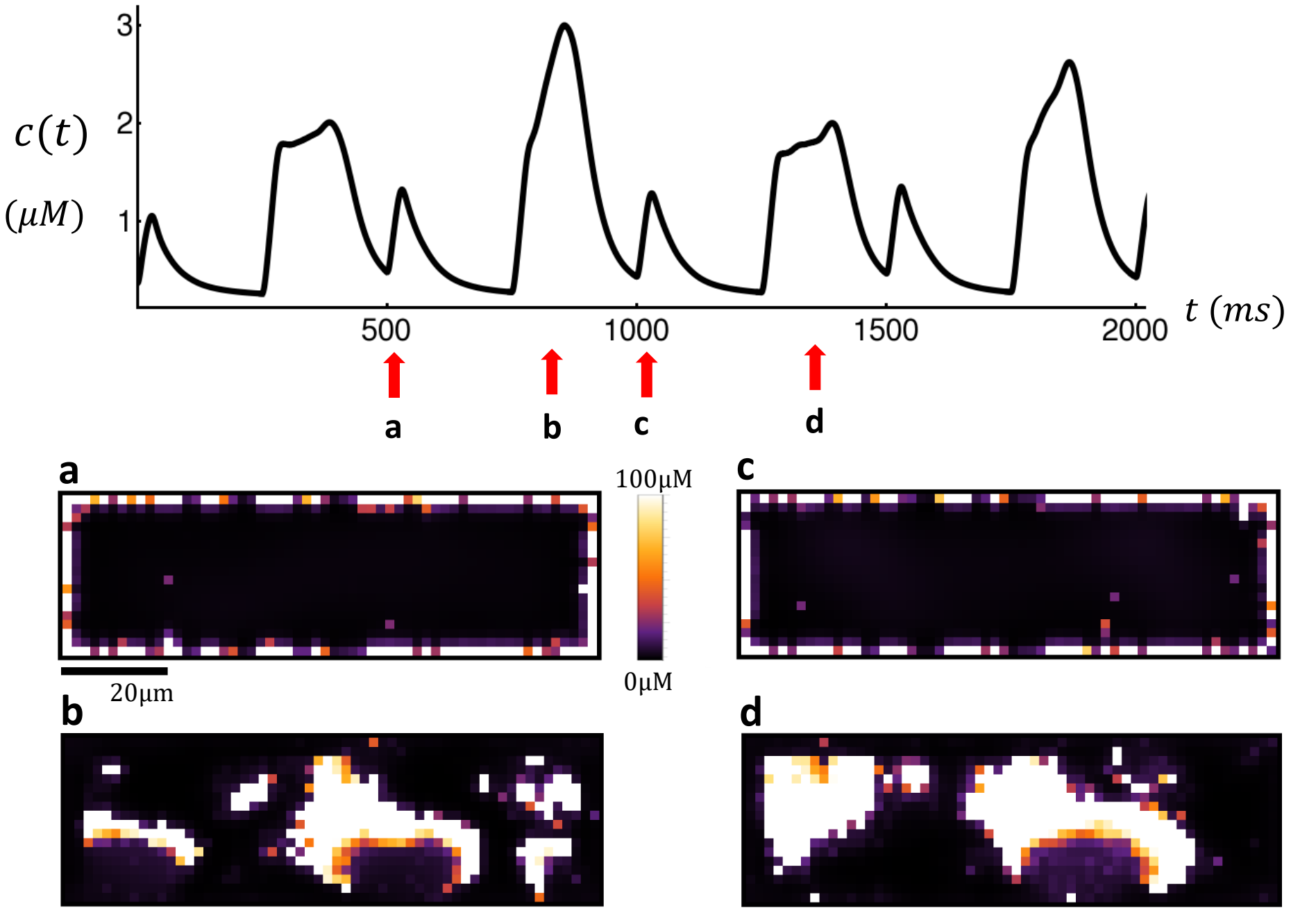

Figure S1

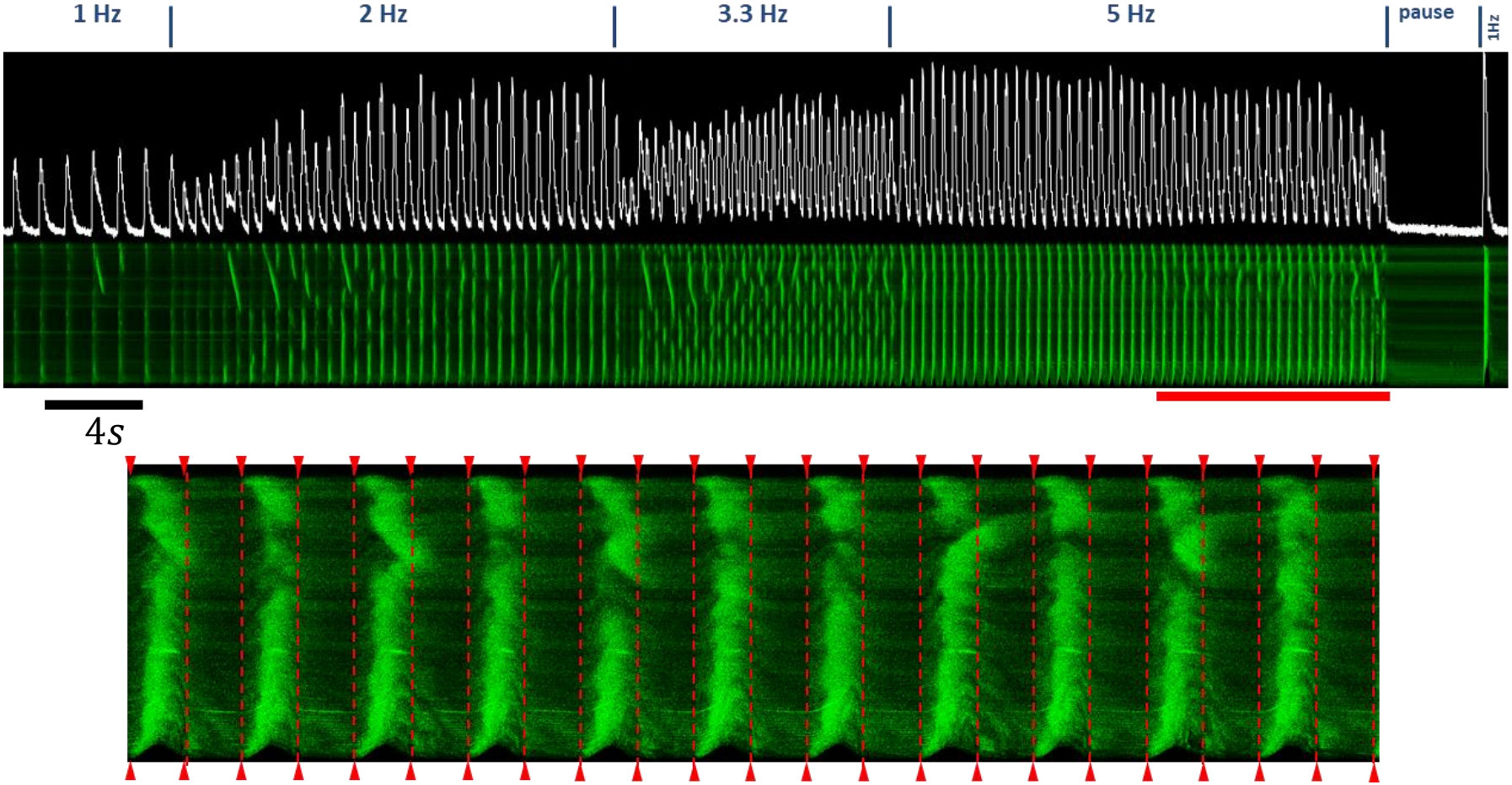

Figure S2